On the Nonsimilarity Boundary-Layer Flows of Second-Order Fluid Over a Stretching Sheet

Xiangcheng You
e-mail: xcyou@sjtu.edu.cn

Hang Xu
e-mail: hangxu@sjtu.edu.cn

Shijun Liao[1]
e-mail: sjliao@sjtu.edu.cn

State Key Laboratory of Ocean Engineering,
School of Naval Architecture, Ocean and Civil Engineering,
Shanghai Jiao Tong University,
Shanghai 200240, China

In this paper, the nonsimilarity boundary-layer flows of second-order fluid over a flat sheet with arbitrary stretching velocity are studied. The boundary-layer equations describing the steady laminar flow of an incompressible viscoelastic fluid past a semi-infinite stretching flat sheet are transformed into a partial differential equation with variable coefficients. An analytic technique for highly nonlinear problems, namely, the homotopy analysis method, is applied to give convergent analytical approximations, which agree well with the numerical results given by the Keller box method. Furthermore, the effects of physical parameters on some important physical quantities, such as the local skin-friction coefficient and the boundary-layer thickness, are investigated in detail. Mathematically, this analytic approach is rather general in principle and can be applied to solve different types of nonlinear partial differential equations with variable coefficients in physics. [DOI: 10.1115/1.3173764]

Keywords: nonsimilarity boundary-layer flow, second-order fluid, series solution, homotopy analysis method

1 Introduction

The flows of an incompressible viscoelastic fluid over a stretching sheet have important applications in the field of industry, such as the extrusion of a polymer sheet from a die or the drawing of plastic films. During the past decades, there has been an increasing interest in the flow behavior of non-Newtonian fluids, especially fluids that exhibit elasticity in shear, these being known as viscoelastic fluids. Beard and Walters [1], in their research of a second-order fluid with the mainstream velocity $U=cx$, proposed a perturbation approach in which the velocity and the pressure of fluid were expanded in a series in terms of a small parameter ε. Rajagopal et al. [2] investigated the boundary-layer flow of a viscoelastic fluid over a stretching sheet, which stretches with velocity $U=cx$, and gave numerical solutions of the nonlinear ordinary differential equation governing the similarity boundary-layer flow in the case of small viscoelastic parameters. Vajravelu et al. [3,4] studied the boundary-layer flow and heat transfer in a viscoelastic fluid over a stretching sheet due to stretching velocity $U=cx$. Sarma and Rao [5] analyzed the heat transfer in the steady laminar flow of an incompressible viscoelastic fluid past a semi-infinite stretching sheet with the same velocity $U=cx$.

Knowledge of non-Newtonian fluid mechanics is still in an early stage, and many aspects of the field have yet to be investigated and clarified in more detail. Most of previous studies of viscoelastic fluids [6–8] only considered the case of the sheet moving with the velocity $U=cx$. For this case, the boundary-layer equations can be reduced to a set of ordinary differential equations with a set of similarity transformations. In nature, the boundary-layer flow over a stretching sheet with the velocity $U=cx$ is not the general model; however, other forms of stretching sheet velocity could lead to nonsimilarity boundary-layer flows. Obviously, it is more meaningful to investigate the nonsimilarity boundary-layer flows.

Currently, a powerful analytic technique for highly nonlinear problems, namely, the homotopy analysis method (HAM) [9–22], has been widely applied to different types of nonlinear problems in science, finance, and engineering. Unlike perturbation techniques, the HAM is independent of any physical parameters so that it is still valid no matter whether or not a nonlinear problem contains small/large physical parameters. Besides, it provides great freedom to choose different base functions to approximate a nonlinear problem so that a better base function can be used to get better approximations. More importantly, different from all other analytic techniques, the HAM provides us with a simple way to ensure the convergence of solution series so that one can always get accurate enough approximations. In this paper, the nonsimilarity boundary-layer flow of a second-order fluid over a stretching sheet with arbitrary stretching velocity is used as an example to propose a general analytic approach for nonsimilarity boundary-layer flows of non-Newtonian fluids.

In Sec. 2, the mathematical description of the nonsimilarity boundary-layer flows is given by means of a nonlinear partial differential equation (PDE). In Sec. 3, the HAM is applied to get convergent series solution of the related nonlinear PDE. The effects of physical parameters on the flows, such as the skin-friction coefficient, the boundary-thickness, and so on, are investigated in Sec. 4. The conclusions and discussions are given in Sec. 5.

2 Mathematical Description

An incompressible homogeneous fluid of second-order [23,24] has a constitutive equation defined by

$$\mathbf{T} = -p\mathbf{I} + \mu\mathbf{A}_1 + \alpha_1\mathbf{A}_2 + \alpha_2\mathbf{A}_1^2 \tag{1}$$

where

$$\mathbf{A}_1 = (\text{grad } \mathbf{v}) + (\text{grad } \mathbf{v})^{\mathbf{T}} \tag{2}$$

[1]Corresponding author.

Contributed by the Applied Mechanics Division of ASME for publication in the JOURNAL OF APPLIED MECHANICS. Manuscript received June 27, 2008; final manuscript received April 15, 2009; published online December 8, 2009. Review conducted by Nesreen Ghaddar.

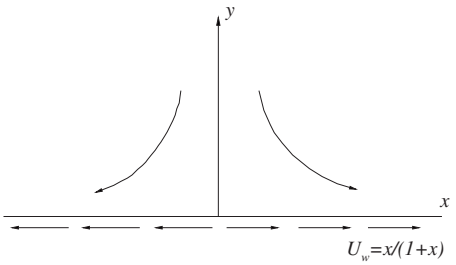

Fig. 1 A sketch of the physical problem

$$\mathbf{A}_2 = d\mathbf{A}_1/dt + \mathbf{A}_1(\text{grad } \mathbf{v}) + (\text{grad } \mathbf{v})^{\mathbf{T}}\mathbf{A}_1 \tag{3}$$

where $\mathbf{T}$ denotes the stress tensor, p, μ, α_1, and α_2 are, respectively, the pressure, the viscosity, and two material constants, $-p\mathbf{I}$ is the spherical stress due to the constraint of incompressibility, $\mathbf{A}_1$ and $\mathbf{A}_2$ are the first two Rivlin–Ericksen tensors, $\mathbf{v}$ denotes the velocity field, and d/dt is the material time derivative.

It is worth mentioning that the sign of α_1 in model equation (1) has been a subject of much controversy; a critical review on this controversial issue has been given a concise discussion by Dunn and Rajagopal [25]. Thus we shall not go into a discussion relating those quarrels but simply follow many researchers by assuming

$$\mu \geq 0, \quad \alpha_1 \geq 0, \quad \alpha_1 + \alpha_2 = 0 \tag{4}$$

As shown in Fig. 1, the two-dimensional boundary-layer flow of a second-order fluid over a stretching flat sheet with an arbitrary stretching velocity $\bar{U}_w(\bar{x})$ is governed by

$$\frac{\partial \bar{u}}{\partial \bar{x}} + \frac{\partial \bar{v}}{\partial \bar{y}} = 0 \tag{5}$$

$$\bar{u}\frac{\partial \bar{u}}{\partial \bar{x}} + \bar{v}\frac{\partial \bar{u}}{\partial \bar{y}} = \nu\frac{\partial^2 \bar{u}}{\partial \bar{y}^2} + \frac{\alpha_1}{\rho}\left[\frac{\partial}{\partial \bar{x}}\left(\bar{u}\frac{\partial^2 \bar{u}}{\partial \bar{y}^2}\right) + \frac{\partial \bar{u}}{\partial \bar{y}}\frac{\partial^2 \bar{v}}{\partial \bar{y}^2} + \bar{v}\frac{\partial^3 \bar{u}}{\partial \bar{y}^3}\right] \tag{6}$$

subject to the following boundary conditions:

$$\bar{u} = \bar{U}_w(\bar{x}), \quad \bar{v} = 0 \quad \text{at} \quad \bar{y} = 0 \tag{7}$$

$$\bar{u} \to 0, \quad \frac{\partial \bar{u}}{\partial \bar{y}} \to 0 \quad \text{as} \quad \bar{y} \to +\infty \tag{8}$$

where $\bar{u}$ and $\bar{v}$ are the velocity components in the $\bar{x}$ and $\bar{y}$ directions, respectively, and ν is the kinematic viscosity, ρ is the density of fluid, and $\bar{U}_w(\bar{x})$ is the stretching velocity of the sheet.

Defining the nondimensional variables,

$$x = \frac{\bar{x}}{L}, \quad y = \text{Re}^{1/2}\left(\frac{\bar{y}}{L}\right), \quad u = \frac{\bar{u}}{U_\infty}, \quad v = \text{Re}^{1/2}\left(\frac{\bar{v}}{U_\infty}\right) \tag{9}$$

where $\text{Re} = U_\infty L/\nu$ is the Reynolds number, Eqs. (5) and (6) can be written in nondimensional form as

$$\frac{\partial u}{\partial x} + \frac{\partial v}{\partial y} = 0 \tag{10}$$

$$u\frac{\partial u}{\partial x} + v\frac{\partial u}{\partial y} = \frac{\partial^2 u}{\partial y^2} + \lambda\left[\frac{\partial}{\partial x}\left(u\frac{\partial^2 u}{\partial y^2}\right) + \frac{\partial u}{\partial y}\frac{\partial^2 v}{\partial y^2} + v\frac{\partial^3 u}{\partial y^3}\right] \tag{11}$$

The boundary conditions become

$$u = U_w(x), \quad v = 0 \quad \text{at} \quad y = 0 \tag{12}$$

$$u \to 0, \quad \frac{\partial u}{\partial y} \to 0 \quad \text{as} \quad y \to +\infty \tag{13}$$

where $\lambda = \alpha_1 U_\infty/\rho\nu L$ is to be interpreted as viscoelastic parameter.

It is well known that in the case of $U_w(x) = cx$, Eqs. (10)–(13) can be reduced to a similarity equation with four boundary conditions by a set of similarity transformations. However, for other stretching velocity, no similarity solutions are available and thus we have to introduce a set of nonsimilarity transformations to convert the original boundary-layer equation to a nonlinear PDE. As far as we know, no one reported such kind of nonsimilarity solutions so far.

Introducing the following variables,

$$\eta = \frac{y}{\sigma(x)}, \quad \psi = \sigma(x) f(x, \eta) \tag{14}$$

where $\psi(x, y)$ denotes a stream function defined in a usual way,

$$u = \frac{\partial \psi}{\partial y}, \quad v = -\frac{\partial \psi}{\partial x} \tag{15}$$

$\sigma(x) > 0$ is a real function of x to be chosen later, such that the continuity equation is automatically satisfied and the momentum equation (11) is transformed to

$$\begin{aligned}\frac{\partial^3 f}{\partial \eta^3} + \frac{1}{2}[\sigma^2(x)]' f\frac{\partial^2 f}{\partial \eta^2} = {} & \sigma^2(x)\left(\frac{\partial f}{\partial \eta}\frac{\partial^2 f}{\partial x\, \partial \eta} - \frac{\partial f}{\partial x}\frac{\partial^2 f}{\partial \eta^2}\right) \\ & - \lambda\left(\frac{\partial^2 f}{\partial x\, \partial \eta}\frac{\partial^3 f}{\partial \eta^3} + \frac{\partial f}{\partial \eta}\frac{\partial^4 f}{\partial x\, \partial \eta^3}\right. \\ & \left. - \frac{\partial^2 f}{\partial \eta^2}\frac{\partial^3 f}{\partial x\, \partial \eta^2} - \frac{\partial f}{\partial x}\frac{\partial^4 f}{\partial \eta^4}\right) \\ & + \frac{2\lambda\sigma'(x)}{\sigma(x)}\left[\frac{\partial f}{\partial \eta}\frac{\partial^3 f}{\partial \eta^3} + \frac{1}{2} f\frac{\partial^4 f}{\partial \eta^4}\right. \\ & \left. - \frac{1}{2}\left(\frac{\partial^2 f}{\partial \eta^2}\right)^2\right]\end{aligned} \tag{16}$$

subject to the boundary conditions

$$f(x,0) = 0, \quad f_\eta(x,0) = U_w(x), \quad f_\eta(x,+\infty) = 0 \tag{17}$$

where f_η denotes the partial derivative with respect to η.

There are an infinite number of sheet velocities $U_w(x)$ that do not satisfy the similarity criteria and thus lead to nonsimilarity boundary-layer flows. Here, without loss of generality, we consider the case $U_w(x) = U_w(\xi)$, where $\xi = \Gamma(x)$ is a given real function of x. By means of the transformation

$$\xi = \Gamma(x) \tag{18}$$

Equation (16) takes the form

$$\begin{aligned}\frac{\partial^3 f}{\partial \eta^3} + \sigma_1(\xi) f\frac{\partial^2 f}{\partial \eta^2} = {} & \sigma_2(\xi)\left(\frac{\partial f}{\partial \eta}\frac{\partial^2 f}{\partial \xi\, \partial \eta} - \frac{\partial f}{\partial \xi}\frac{\partial^2 f}{\partial \eta^2}\right) + \sigma_3(\xi) \\ & \times\left(\frac{\partial^2 f}{\partial \xi\, \partial \eta}\frac{\partial^3 f}{\partial \eta^3} + \frac{\partial f}{\partial \eta}\frac{\partial^4 f}{\partial \xi\, \partial \eta^3} - \frac{\partial^2 f}{\partial \eta^2}\frac{\partial^3 f}{\partial \xi\, \partial \eta^2}\right. \\ & \left. - \frac{\partial f}{\partial \xi}\frac{\partial^4 f}{\partial \eta^4}\right) + \sigma_4(\xi)\left[\frac{\partial f}{\partial \eta}\frac{\partial^3 f}{\partial \eta^3} + \frac{1}{2} f\frac{\partial^4 f}{\partial \eta^4}\right. \\ & \left. - \frac{1}{2}\left(\frac{\partial^2 f}{\partial \eta^2}\right)^2\right]\end{aligned} \tag{19}$$

subject to the boundary conditions

$$f(\xi,0) = 0, \quad f_\eta(\xi,0) = U_w(\xi), \quad f_\eta(\xi,+\infty) = 0 \tag{20}$$

where

$$\sigma_1(\xi) = \frac{1}{2}[\sigma^2(x)]', \quad \sigma_2(\xi) = \Gamma'(x)\sigma^2(x),$$

$$\sigma_3(\xi) = -\lambda\Gamma'(x), \quad \sigma_4(\xi) = \frac{2\lambda\sigma'(x)}{\sigma(x)} \tag{21}$$

in which x is expressed by ξ, i.e., $x=\Gamma^{-1}(\xi)$.

It is also worth mentioning that the above mentioned analysis is valid for various stretching velocity distributions. While owing the restriction of similarity (or nonsimilarity) method, many velocity distributions may not produce the equation, which admit exact solutions in the whole regions $0\le x<\infty$ and $0\le y<\infty$.

For convenience, we choose

$$U_w(x) = \frac{x}{1+x}$$

as the example; note that $U_w \to x$ as $x \to 0$, and $U_w \to 1$ as $x \to +\infty$, respectively. From practical points of view, this is reasonable because $U_w(x)$ is always bounded in practice.

For the special case of $\lambda=0$, corresponding to Newtonian fluid, the flows near $x=0$ should be close to the similarity ones in the case of $U_w=x$, and besides, the flows at $x\to+\infty$ should be close to the similarity ones in the case of $U_w=1$, respectively. For these similarity flows of Newtonian fluid, it is well known that the corresponding similarity variables are $\bar{y}/\sqrt{\nu}$ in the case of $U_w=x$ and $\bar{y}/\sqrt{\nu\bar{x}}$ in the case of $U_w=1$, respectively. Besides, there exist the similarity boundary-layer flows of non-Newtonian fluid (i.e., $\lambda\neq 0$) only in the case of $U_w=x$ with the corresponding similarity variable $\eta=\bar{y}/\sqrt{\nu}$. It is very interesting that, in the case of $U_w=x$, the similarity boundary-layer flows of both Newtonian and non-Newtonian fluids have the *same* similarity variable $\eta=\bar{y}/\sqrt{\nu}$. Considering all of the above facts, and due to the definition (14) of the variable η, it is natural for us to choose

$$\sigma(x) = \sqrt{1+x} \tag{22}$$

so that for the nonsimilarity flows of non-Newtonian fluid, η tends to $\bar{y}/\sqrt{\nu}$ as $x\to 0$, and to $\bar{y}/\sqrt{\nu\bar{x}}$ as $x\to+\infty$, respectively. In this way, our analytic approach is also valid for similarity boundary-layer flows of Newtonian fluid ($\lambda=0$) and non-Newtonian fluid in the case of $U_w=x$. Such kind of theoretical consistency is very important, especially in the case of lack of experimental data.

It is natural for us to define

$$\xi = \Gamma(x) = \frac{x}{1+x} \tag{23}$$

which gives

$$U_w = \xi, \quad \sigma_1(\xi) = \frac{1}{2}, \quad \sigma_2(\xi) = 1-\xi,$$

$$\sigma_3(\xi) = -\lambda(1-\xi)^2, \quad \sigma_4(\xi) = \lambda(1-\xi) \tag{24}$$

Then the governing equation is transformed into

$$\frac{\partial^3 f}{\partial \eta^3} + \frac{1}{2} f \frac{\partial^2 f}{\partial \eta^2} = (1-\xi)\left(\frac{\partial f}{\partial \eta}\frac{\partial^2 f}{\partial \xi\, \partial\, \eta} - \frac{\partial f}{\partial \xi}\frac{\partial^2 f}{\partial \eta^2}\right) - \lambda(1-\xi)^2\left(\frac{\partial^2 f}{\partial \xi\, \partial\, \eta}\frac{\partial^3 f}{\partial \eta^3} + \frac{\partial f}{\partial \eta}\frac{\partial^4 f}{\partial \xi\, \partial\, \eta^3} - \frac{\partial^2 f}{\partial \eta^2}\frac{\partial^3 f}{\partial \xi\, \partial\, \eta^2} - \frac{\partial f}{\partial \xi}\frac{\partial^4 f}{\partial \eta^4}\right) + \lambda(1-\xi)\left[\frac{\partial f}{\partial \eta}\frac{\partial^3 f}{\partial \eta^3} + \frac{1}{2} f \frac{\partial^4 f}{\partial \eta^4} - \frac{1}{2}\left(\frac{\partial^2 f}{\partial \eta^2}\right)^2\right] \tag{25}$$

subject to the boundary conditions

$$f(\xi,0) = 0, \quad f_\eta(\xi,0) = \xi, \quad f_\eta(\xi,+\infty) = 0 \tag{26}$$

Note that the partial differential equation (25) contains only one linear term $f_{\eta\eta\eta}$, and thus is highly nonlinear. Such kind of nonlinear PDE is hard to solve, especially by means of analytic methods.

3 The Analytic Approach Based on the HAM

From physical points of view, it is well known that most of boundary-layer flows decay exponentially at infinity. Thus, it is reasonable to assume that $f(\xi,\eta)$ could be expressed by the following set of functions:

$$\{\xi^k \eta^m \exp(-n\eta) | k \ge 0, m \ge 0, n \ge 0\} \tag{27}$$

such that

$$f(\xi,\eta) = \sum_{k=0}^{+\infty}\sum_{m=0}^{+\infty}\sum_{n=0}^{+\infty} a_k^{m,n} \xi^k \eta^m \exp(-n\eta) \tag{28}$$

where $a_k^{m,n}$ is a coefficient. It provides us the so-called solution expression, which plays an important role in the frame of the HAM, as shown later.

Using the solution expression (28) and considering the boundary conditions (26), it is convenient to select the initial guess

$$f_0(\xi,\eta) = U_w(\xi)[1-\exp(-\eta)] \tag{29}$$

and the auxiliary linear operator,

$$\mathcal{L}[\Phi(\xi,\eta;q)] = \frac{\partial^3 \Phi}{\partial \eta^3} + \frac{\partial^2 \Phi}{\partial \eta^2} \tag{30}$$

which has the property

$$\mathcal{L}[C_0 + C_1 \exp(-\eta) + C_2 \eta] = 0 \tag{31}$$

where C_0, C_1, and C_2 are the integral coefficients and using $q \in [0,1]$ as an embedding parameter. Then, based on Eq. (25), we define the nonlinear operator

$$\mathcal{N}[\Phi(\xi,\eta;q)] = \left(\frac{\partial^3 \Phi}{\partial \eta^3} + \frac{1}{2}\Phi\frac{\partial^2 \Phi}{\partial \eta^2}\right) - (1-\xi)\left(\frac{\partial \Phi}{\partial \eta}\frac{\partial^2 \Phi}{\partial \xi\, \partial\, \eta} - \frac{\partial \Phi}{\partial \xi}\frac{\partial^2 \Phi}{\partial \eta^2}\right) + \lambda(1-\xi)^2\left(\frac{\partial^2 \Phi}{\partial \xi\, \partial\, \eta}\frac{\partial^3 \Phi}{\partial \eta^3} + \frac{\partial \Phi}{\partial \eta}\frac{\partial^4 \Phi}{\partial \xi\, \partial\, \eta^3} - \frac{\partial^2 \Phi}{\partial \eta^2}\frac{\partial^3 \Phi}{\partial \xi\, \partial\, \eta^2} - \frac{\partial \Phi}{\partial \xi}\frac{\partial^4 \Phi}{\partial \eta^4}\right) - \lambda(1-\xi)\left[\frac{\partial \Phi}{\partial \eta}\frac{\partial^3 \Phi}{\partial \eta^3} + \frac{1}{2}\Phi\frac{\partial^4 \Phi}{\partial \eta^4} - \frac{1}{2}\left(\frac{\partial^2 \Phi}{\partial \eta^2}\right)^2\right] \tag{32}$$

Let $\hbar$ denote a nonzero auxiliary parameter. We construct the zeroth-order deformation equation,

$$(1-q)\mathcal{L}[\Phi(\xi,\eta;q) - f_0(x,y)] = q\hbar\mathcal{N}[\Phi(\xi,\eta;q)] \tag{33}$$

subject to the boundary conditions

$$\Phi(\xi,0;q) = 0, \qquad \left.\frac{\partial \Phi(\xi,\eta;q)}{\partial \eta}\right|_{\eta=0} = \xi, \qquad \left.\frac{\partial \Phi(\xi,\eta;q)}{\partial \eta}\right|_{\eta=+\infty} = 0 \tag{34}$$

When $q=0$ and $q=1$, we have

$$\Phi(\xi,\eta;0) = f_0(\xi,\eta), \quad \Phi(\xi,\eta;1) = f(\xi,\eta) \tag{35}$$

Thus, as q increases from 0 to 1, $\Phi(\xi,\eta;q)$ varies from the initial guess $f_0(\xi,\eta)$ to the exact solution $f(\xi,\eta)$ of Eqs. (25) and (26). Then, by Taylor's theorem, we expand $\Phi(\xi,\eta;q)$ in the power series

$$\Phi(\xi,\eta;q) = \Phi(\xi,\eta;0) + \sum_{n=1}^{+\infty} f_n(\xi,\eta) q^n \tag{36}$$

where

$$f_n(\xi,\eta)=\frac{1}{n!}\left.\frac{\partial^n\Phi(\xi,\eta;q)}{\partial q^n}\right|_{q=0} \tag{37}$$

Assuming that all of them are correctly chosen so that the series (Eq. (36)) converges at $q=1$, we then have from Eq. (34) that

$$f(\xi,\eta)=f_0(\xi,\eta)+\sum_{n=1}^{+\infty}f_n(\xi,\eta) \tag{38}$$

write

$$\boldsymbol{f}_n=\{f_0,f_1,f_2,\ldots,f_n\}$$

Differentiating the HAM deformation equations (33) and its boundary conditions m times with respect to q, then dividing by $m!$, and finally setting $q=0$, we have the mth-order deformation equations,

$$\mathcal{L}[f_m(\xi,\eta)-\chi_m f_{m-1}(\xi,\eta)]=\hbar R_m(\boldsymbol{f}_{m-1},\xi) \tag{39}$$

subject to the boundary conditions

$$f_m(\xi,0)=0,\qquad \left.\frac{\partial f_m(\xi,\eta)}{\partial\eta}\right|_{\eta=0}=0,\qquad \left.\frac{\partial f_m(\xi,\eta;q)}{\partial\eta}\right|_{\eta=+\infty}=0 \tag{40}$$

where

$$\begin{aligned}R_m(\boldsymbol{f}_{m-1},\xi)=&\left(\frac{\partial^3 f_{m-1}}{\partial\eta^3}+\frac{1}{2}\sum_{n=0}^{m-1}f_{m-1-n}\frac{\partial^2 f_n}{\partial\eta^2}\right)\\&-(1-\xi)\sum_{n=0}^{m-1}\left(\frac{\partial f_{m-1-n}}{\partial\eta}\frac{\partial^2 f_n}{\partial\xi\,\partial\eta}-\frac{\partial f_{m-1-n}}{\partial\xi}\frac{\partial^2 f_n}{\partial\eta^2}\right)\\&+\lambda(1-\xi)^2\sum_{n=0}^{m-1}\left(\frac{\partial^2 f_{m-1-n}}{\partial\xi\,\partial\eta}\frac{\partial^3 f_n}{\partial\eta^3}+\frac{\partial f_{m-1-n}}{\partial\eta}\frac{\partial^4 f_n}{\partial\xi\,\partial\eta^3}\right)\\&-\lambda(1-\xi)^2\sum_{n=0}^{m-1}\left(\frac{\partial^2 f_{m-1-n}}{\partial\eta^2}\frac{\partial^3 f_n}{\partial\xi\,\partial\eta^2}+\frac{\partial f_{m-1-n}}{\partial\xi}\frac{\partial^4 f_n}{\partial\eta^4}\right)\\&-\lambda(1-\xi)\sum_{n=0}^{m-1}\left(\frac{\partial f_{m-1-n}}{\partial\eta}\frac{\partial^3 f_n}{\partial\eta^3}+\frac{1}{2}f_{m-1-n}\frac{\partial^4 f_n}{\partial\eta^4}\right.\\&\left.-\frac{1}{2}\frac{\partial^2 f_{m-1-n}}{\partial\eta^2}\frac{\partial^2 f_n}{\partial\eta^2}\right)\end{aligned} \tag{41}$$

and

$$\chi_m=\begin{cases}1, & m>1\\ 0, & m=1\end{cases} \tag{42}$$

Let $f_m^*(\xi,\eta)$ denote a particular solution of Eq. (39). In Eq. (31), its general solution reads

$$f_m(\xi,\eta)=f_m^*(\xi,\eta)+C_0^m+C_1^m\exp(-\eta) \tag{43}$$

where the coefficients C_0^m and C_1^m are determined by the boundary conditions (40). In this way, it is easy to solve the linear equations of Eqs. (39) and (40) successively.

Note that the right-hand side of Eq. (39) can be regarded as a known term, and its left-hand side is independent of ξ. Thus, Eq. (39) is, in fact, an ordinary differential equation (ODE) about η. Therefore, the original *nonlinear* partial differential equation (25) is transferred into an infinite number of *linear* ordinary differential equations that are much easier to solve. Note that, different from perturbation techniques, such kind of transformation does not need any small physical parameters. Besides, it should be emphasized that the chosen auxiliary linear operator (30) has not a close relationship with the linear term $f_{\eta\eta\eta}$ in the original equation (25). This is mainly because, different from all of other analytic techniques, the homotopy analysis method provides us with great freedom to choose the auxiliary linear operator. Without such kind of freedom, it is impossible for us to get such kind of series solution convergent in the whole spatial region $0\le x<+\infty$ and $0\le y<+\infty$.

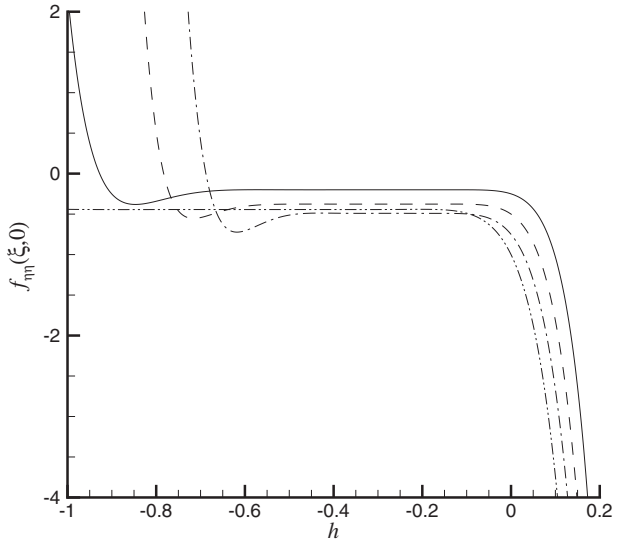

Fig. 2 The curves $f_{\eta\eta}(\xi,0)\sim\hbar$ at the 15th-order of approximation in the case of $\lambda=1/2$. Solid line: $\xi=1/4$, dashed line: $\xi=1/2$, dash-dotted line: $\xi=3/4$, and dash-dot-dotted line: $\xi=1$.

4 Result Analysis

With the help of the HAM, it is easy to give analytical approximations for Eq. (25) in the following form:

$$f(\xi,\eta)=\sum_{m=0}^{M}f_m(\xi,\eta) \tag{44}$$

Using symbolic computation software (such as MATHEMATICA), it is easy to solve the high-order deformation equations (39) and (40). Obviously, it is important to ensure the convergence of the solution series (36) for all possible physical variables $0\le x<+\infty$ and $0\le y<+\infty$. Note that the series solution (36) contains an auxiliary parameter $\hbar$, which provides a simple way to adjust and control the convergence region and rate of series solution, as mentioned by Liao and co-worker [10,11,14]. Mathematically, $f_{\eta\eta}(\xi,0)$ is dependent on both of the physical variable ξ and the auxiliary parameter $\hbar$. So, from mathematical view points, given a value of ξ, $f_{\eta\eta}(\xi,0)$ is a power series of $\hbar$ and thus its convergence is determined by $\hbar$. However, from physical view points, for a given value of ξ, the local coefficient of skin friction is unique; i.e., there should exist only one value of $f_{\eta\eta}(\xi,0)$ (we assume here that no multiple solutions exist). Therefore, for a given value of ξ, the corresponding series solution of $f_{\eta\eta}(\xi,0)$ given by different values of $\hbar$ should converge to the same value, as long as it is not divergent. This is indeed true. For example, in the case of $\lambda=1/2$, regarding $\hbar$ as a variable, we can plot the curves of $f_{\eta\eta}(\xi,0)\sim\hbar$ for different values of ξ varying from 0 to 1, as shown in Fig. 2. Obviously, for any a given value of $\xi\in[0,1]$, $f_{\eta\eta}(\xi,0)$ converges to the same value in the case of $\hbar\in[-2/5,-1/10]$. Thus, if we choose a value of $\hbar$ in the region $-2/5\le\hbar\le-1/10$, we get the series solution of $f_{\eta\eta}(\xi,0)$ convergent in the whole region $\xi\in[0,1]$. For example, in the case of $\hbar=-1/5$, our HAM approximations of $f_{\eta\eta}(\xi,0)$ agree well with the numerical results given by the Keller-box method [26] in the whole region $\xi\in[0,1]$, as shown in Table 1 and Fig. 3. With the Keller-box scheme, the computational domain of η, ranged from 0 to 10, is divided into 1000 intervals, while the domain ξ, ranged from 0 to 1, is divided into 100 time steps. Fixed step sizes are

Table 1 Value of $f''(\xi,0)$ in the case of $\lambda=1/2$ by means of $\hbar=-1/5$

ξ	20th HAM approximation	Numerical result	Relative error (%)
0	0	0	0
0.1	−0.08122	−0.08178	0.69
0.2	−0.16094	−0.16136	0.26
0.3	−0.23796	−0.23822	0.11
0.4	−0.31062	−0.31073	0.04
0.5	−0.37663	−0.37659	0.01
0.6	−0.43294	−0.43278	0.04
0.7	−0.4756	−0.47534	0.05
0.8	−0.49975	−0.49943	0.06
0.9	−0.49909	−0.49856	0.11
1.0	−0.44269	−0.44495	0.51

employed in both directions. The convergence criterion used is based on the root mean square error (rms), which is 1×10^{-6} in the present work.

The convergence of the series of $f_{\eta\eta}(\xi,0)$ can be accelerated by means of homotopy-Padé technique, as shown in Table 2. It should be emphasized that, when $\hbar\notin[-2/5,-1/10]$ such as $\hbar=-1/2$ or $\hbar=-3/5$, the series solution of $f_{\eta\eta}(\xi,0)$ converges only for small ξ and $\xi=1$, corresponding to small x and $x\to+\infty$, respectively, but diverges for some values of ξ, as shown in Fig. 3. So, it is very important to choose a proper value of the auxiliary parameter $\hbar$, and the curve $f_{\eta\eta}(\xi,0)\sim\hbar$ indeed provides us a simple way to do so. Furthermore, it is found that, as long as the series of $f_{\eta\eta}(\xi,0)$ is convergent in the region $\xi\in[0,1]$, the corresponding series of $f(\xi,\eta)$, $f_\eta(\xi,\eta)$, and so on, given by the same value of $\hbar$, are also convergent in the *whole* regions $0\le\xi\le1$ and $0\le\eta<+\infty$, corresponding to $0\le x<+\infty$ and $0\le y<+\infty$. For example, in the case of $\hbar=-1/5$, the series solution of $f_\eta(\xi,\eta)$ converges in the whole regions of the spatial variables, as shown in Fig. 4. Thus, it is the auxiliary parameter $\hbar$ that indeed provides us a simple way to control and adjust the convergence of the series solution. This is an obvious advantage of the homotopy analysis method, compared with all of other analytic techniques. Thus, the curves $f_{\eta\eta}(\xi,0)\sim\hbar$ are indeed straightforward and helpful in choosing a proper value of the auxiliary parameter $\hbar$.

Note that $\hbar=-1$ gives divergent series solution. It should be emphasized that, as proved by Liao [10], other nonperturbation techniques such as Adomian's decomposition method [27], the δ-perturbation method [28,29], and Lyapunov's artificial small parameter method [30] are special cases of the homotopy analysis method in the case of $\hbar=-1$. So, if these nonperturbation methods are used here, one cannot get convergent series solution valid in the whole regions $0\le x<+\infty$ and $0\le y<+\infty$.

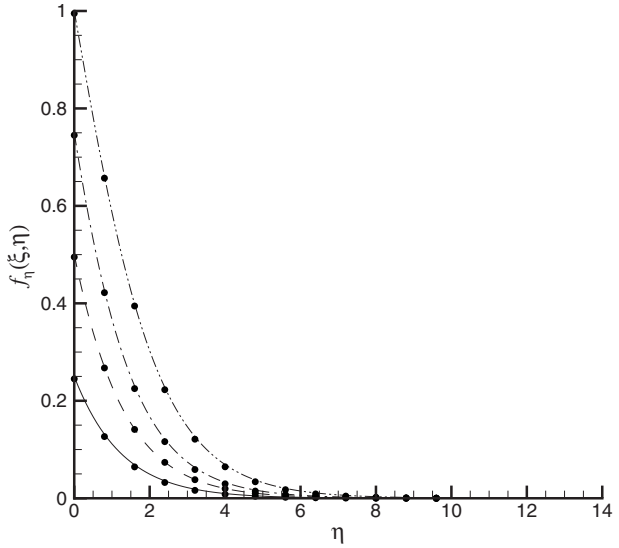

Fig. 4 The curves of $f_\eta(\xi,\eta)$ in the case of $\lambda=1/2$ by means of $\hbar=-1/5$. Solid line: $\xi=1/4$, dashed line: $\xi=1/2$, dash-dotted line: $\xi=3/4$, dash-dot-dotted line: $\xi=1$, and symbols: numerical results.

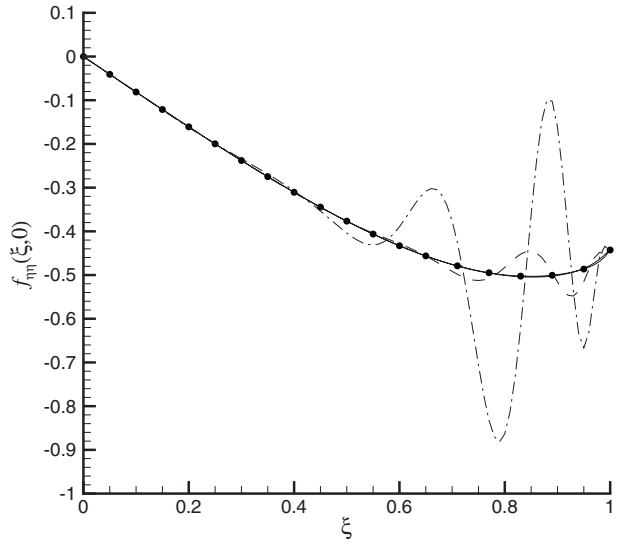

Fig. 3 The curves of $f_{\eta\eta}(\xi,0)\sim\xi$ in the case of $\lambda=1/2$ by means of different values of $\hbar$. Solid line: 20th-order HAM result when $\hbar=-1/5$, symbols: 25th-order HAM result when $\hbar=-1/5$, dashed line: 20th-order HAM result when $\hbar=-1/2$, and dash-dotted line: 20th-order HAM result when $\hbar=-3/5$.

Table 2 The (m,m) homotopy-Padé approximation of $f''(\xi,0)$ in the case of $\lambda=1/2$

ξ	$m=2$	$m=4$	$m=6$	$m=8$	$m=10$
0	0	0	0	0	0
0.1	−0.08150	−0.08123	−0.08122	−0.08122	−0.08122
0.2	−0.16175	−0.16099	−0.16095	−0.16094	−0.16094
0.3	−0.23958	−0.23809	−0.23891	−0.23797	−0.23797
0.4	−0.31334	−0.31075	−0.31072	−0.31056	−0.31063
0.5	−0.38122	−0.37689	−0.37671	−0.37663	−0.37664
0.6	−0.44073	−0.43415	−0.43330	−0.43305	−0.43299
0.7	−0.48943	−0.48129	−0.47941	−0.47872	−0.47855
0.8	−0.52449	−0.53338	−0.51159	−0.49251	−0.49591
0.9	−0.53671	−0.43247	−0.47158	−0.49151	−0.49161
1.0	−0.45737	−0.44458	−0.44380	−0.44375	−0.44375

The physical quantities of interest are the local coefficient of skin friction $C_f(\bar{x})$ and the boundary-layer thickness $\delta(\bar{x})$, which are defined by

$$C_f(\bar{x}) = \frac{\tau_{\bar{x}\bar{y}}|_{\bar{y}\to 0}}{\rho \bar{U}_w^2(\bar{x})/2} \tag{45}$$

and

$$\delta(\bar{x}) = \frac{1}{\bar{U}_w(\bar{x})} \int_{\bar{y}=0}^{+\infty} \bar{u}(\bar{x},\bar{y}) d\bar{y} \tag{46}$$

respectively.

Then the quantities of the local skin-friction coefficient $C_f^*(x)$ and the boundary-layer thickness $\delta^*(x)$ are, respectively, denoted by

$$C_f^*(x) = C_f(\bar{x})\mathrm{Re}^{1/2} = \frac{1}{\rho U_w^2(x)/2}\left[\mu\frac{\partial u}{\partial y} + 2\alpha_1\left(u\frac{\partial^2 u}{\partial x\,\partial y} + 2\frac{\partial u}{\partial x}\frac{\partial u}{\partial y}\right)\right]\Bigg|_{y\to 0} = \frac{2}{\sigma(x)U_w^2(x)}\left\{\frac{\partial^2 f}{\partial \eta^2} + 2\lambda\left[\frac{\partial f}{\partial \eta}\left(\frac{\partial^3 f}{\partial x\,\partial \eta^2} - \frac{\sigma'(x)}{\sigma(x)}\frac{\partial^2 f}{\partial \eta^2}\right) + 2\frac{\partial^2 f}{\partial \eta^2}\frac{\partial^2 f}{\partial x\,\partial \eta}\right]\right\}\Bigg|_{\eta\to 0} \tag{47}$$

$$\delta^*(x) = \delta(\bar{x})\mathrm{Re}^{1/2}/L = \frac{1}{U_w(x)}\int_0^{+\infty} u(x,y)dy \tag{48}$$

In Eq. (47), it is found that the local skin-friction coefficient $C_f^*(x)$ of the boundary-layer flows is related to $f_{\eta\eta}(x,0), f_\eta(x,0), f_{x\eta\eta}(x,0), f_{x\eta}(x,0)$. Here x can be expressed by ξ, i.e., $x=\Gamma^{-1}(\xi)$. For example, in the case of $\lambda=1/2$ by means of $\hbar=-1/5$, our 20th-order HAM approximation for $f_{\eta\eta}(\xi,0)$ reads

$$\begin{aligned} f_{\eta\eta}(\xi,0) = &-0.816495\xi + 0.0298867\xi^2 + 0.122633\xi^3 + 0.098815\xi^4 \\ &+ 0.064059\xi^5 + 0.0348928\xi^6 + 0.0141632\xi^7 \\ &+ 0.00185689\xi^8 - 0.00462037\xi^9 - 0.00696416\xi^{10} \\ &- 0.00599676\xi^{11} + 0.00952493\xi^{12} - 1.18932\xi^{13} \\ &+ 52.0483\xi^{14} - 1358.02\xi^{15} + 23131.6\xi^{16} - 274704\xi^{17} \\ &+ 2.38646\times 10^6\xi^{18} - 1.57216\times 10^7\xi^{19} + 8.07306 \\ &\times 10^7\xi^{20} + 3.30116\times 10^8\xi^{21} + 1.09325\times 10^9\xi^{22} \\ &- 2.97188\times 10^9\xi^{23} + 6.70295\times 10^9\xi^{24} - 1.26504 \\ &\times 10^{10}\xi^{25} + 2.01092\times 10^{10}\xi^{26} - 2.70542\times 10^{10}\xi^{27} \\ &+ 3.09047\times 10^{10}\xi^{28} - 3.00256\times 10^{10}\xi^{29} + 2.48125 \\ &\times 10^{10}\xi^{30} - 1.74125\times 10^{10}\xi^{31} + 1.03405\times 10^{10}\xi^{32} \\ &- 5.16676\times 10^9\xi^{33} + 2.15366\times 10^9\xi^{34} - 7.39776 \\ &\times 10^8\xi^{35} + 2.05785\times 10^8\xi^{36} - 4.51997\times 10^7\xi^{37} \\ &+ 7.54546\times 10^6\xi^{38} - 899{,}667\xi^{39} + 68254.7\xi^{40} \\ &- 2476.2\xi^{41} \end{aligned} \tag{49}$$

which agrees well with the 25th-order approximations and is accurate in the whole region $0\le\xi\le 1$, i.e., $0\le x<+\infty$. Knowing the accurate values of $f_{\eta\eta}(x,0), f_\eta(x,0)$ and $f_{x\eta\eta}(x,0), f_{x\eta}(x,0)$, it is straightforward to calculate the local skin-friction coefficient $C_f(x)$ by means of Eq. (47). It is found that, in the case of $\lambda=1/2$, $C_f^*(x)$ tends to $-6.53215/x$ as $x\to 0$ and $-0.881819/\sqrt{x}$ as $x\to+\infty$, respectively, as shown in Fig. 5. Besides, in the case of $U_w=\xi$ and $\lambda=1/2$, $\delta^*(x)$ tends to 1.22472 as $x\to 0$ and $1.62805\sqrt{x}$ as $x\to+\infty$, respectively, as shown in Fig. 6. The curves of $C_f^*(x)$ and $\delta^*(x)$ at different values of λ are shown in Figs. 7 and 8. It is

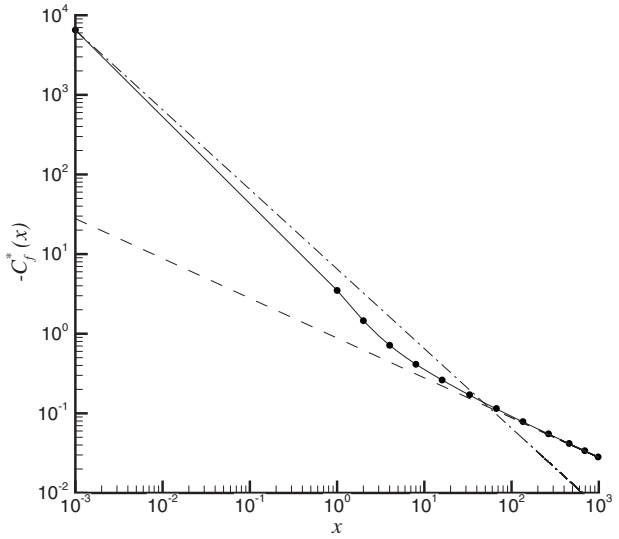

Fig. 5 $C_f^*(x)$ in the case of $\lambda=1/2$ by means of $\hbar=-1/5$. Solid line: 20th-order HAM approximation, symbols: 20th-order HAM approximation, dashed line: $C_f^*(x)=-0.881819/\sqrt{x}$, and dash-dotted line: $C_f^*(x)=-6.53215/x$.

interesting that, as $x\to+\infty$, the local skin-friction coefficient $C_f^*(x)$ tends to the same *asymptotic* expression $-0.881819/\sqrt{x}$ for *all different* values of λ, as shown in Table 3. This is mainly because $\sigma'(x)\to 0$ and

$$\frac{\partial^2 f}{\partial x\,\partial \eta} \sim \frac{1}{\sqrt{x}}, \quad \frac{\partial^3 f}{\partial x\,\partial \eta^2} \sim \frac{1}{\sqrt{x}}$$

as $x\to+\infty$. Thus, according to Eq. (47), all terms of $C_f^*(x)$ related to λ tend to zero as $x\to+\infty$. Similarly, it is found that, as $x\to+\infty$, the boundary-layer thickness $\delta^*(x)$ tends to the *same* asymptotic expression $1.62805\sqrt{x}$ for all different values of λ, as shown in Table 4. Near $x=0$, the local skin-friction coefficient $C_f^*(x)$ adds with the increase in λ and the boundary-layer thick-

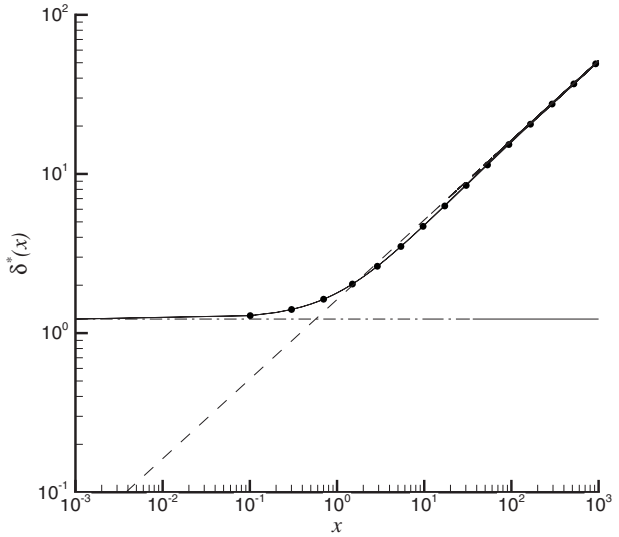

Fig. 6 $\delta^*(x)$ in the case of $\lambda=1/2$ by means of $\hbar=-1/5$. Solid line: 20th-order HAM approximation, symbols: 25th-order HAM approximation, dashed line: $\delta^*(x)=1.62805\sqrt{x}$, and dash-dotted line: $\delta^*(x)=1.22472$.

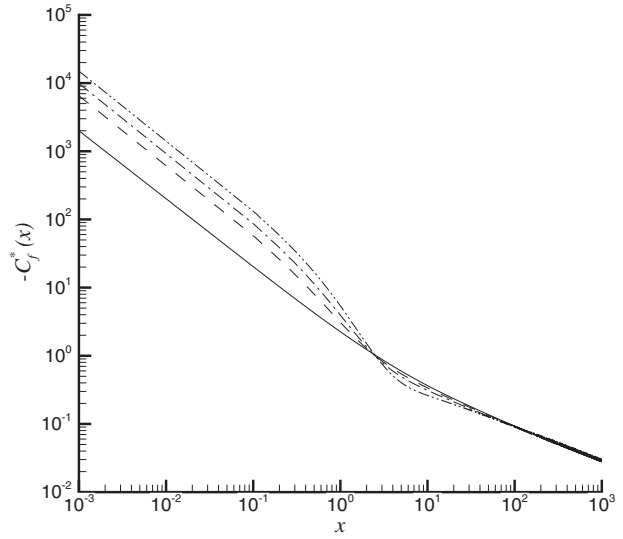

Fig. 7 The 20th-order HAM approximation of $C_f^*(x)$ at different values of λ. Solid line: λ=0, dashed line: λ=1/2, dash-dotted line: λ=1, and dash-dot-dotted line: λ=2.

ness $\delta^*(x)$ has the same change with the augment of λ, as shown in Figs. 7 and 8, respectively.

If the velocity distribution

$$U_w = \alpha\frac{x}{1+x} + (1-\alpha)\left(\frac{x}{1+x}\right)^2 \tag{50}$$

is applied, the resulting governing equations contain exact solution in the whole regions $0 \le x < \infty$ and $0 \le y < \infty$ as well. Here α

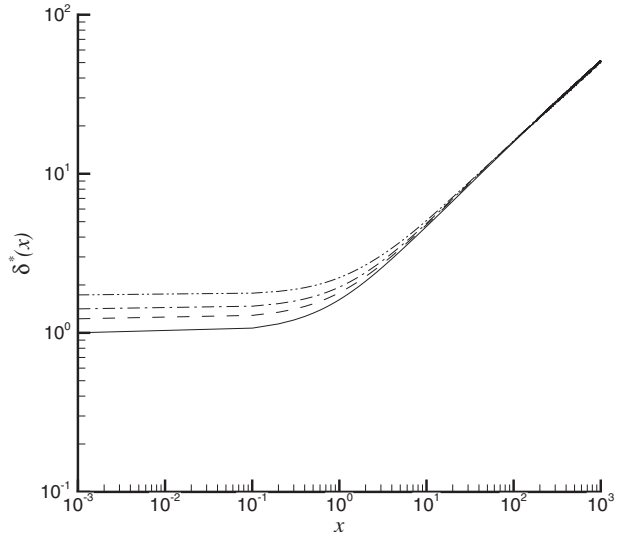

Fig. 8 The 20th-order HAM approximation of $\delta^*(x)$ at different values of λ. Solid line: λ=0, dashed line: λ=1/2, dash-dotted line: λ=1, and dash-dot-dotted line: λ=2.

Table 3 $C_f^*(x)$ at some values of λ

λ	$\hbar$	$x \to 0$	$x \to +\infty$
0	−1/5	$-2/x$	$-0.881819/\sqrt{x}$
1/2	−1/5	$-6.53215/x$	$-0.881819/\sqrt{x}$
1	−1/5	$-9.8984/x$	$-0.881819/\sqrt{x}$
2	−1/8	$-15.0044/x$	$-0.881819/\sqrt{x}$

Table 4 $\delta^*(x)$ at some values of λ

λ	$\hbar$	$x \to 0$	$x \to +\infty$
0	−1/5	1	$1.62805\sqrt{x}$
1/2	−1/5	1.22472	$1.62805\sqrt{x}$
1	−1/5	1.41419	$1.62805\sqrt{x}$
2	−1/8	1.73205	$1.62805\sqrt{x}$

is a parameter, which is used to control the velocity distribution U_w, as shown in Fig. 9. For this case, it is found that the boundary-layer thickness $\delta^*(x)$ increases as α decreases, as shown in Fig. 10.

Similarly, if the velocity distributions of the form

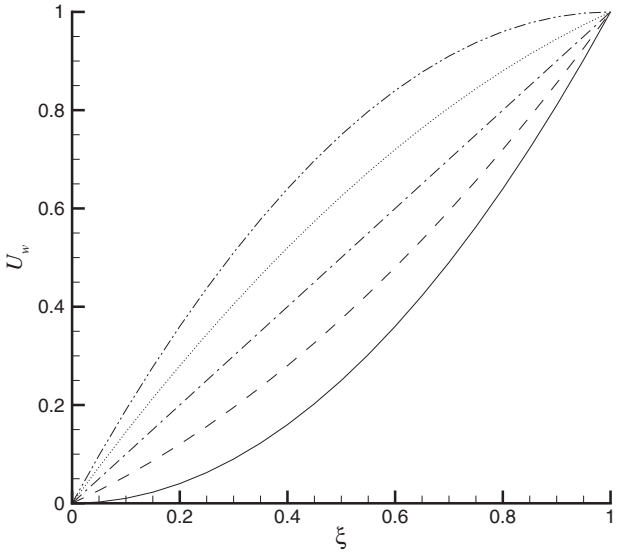

Fig. 9 The $U_w(\xi)$ at different values of α. Solid line: α=0, dashed line: α=1/2, dash-dotted line: α=1, dotted line: α=3/2, and dash-dot-dotted line: α=2.

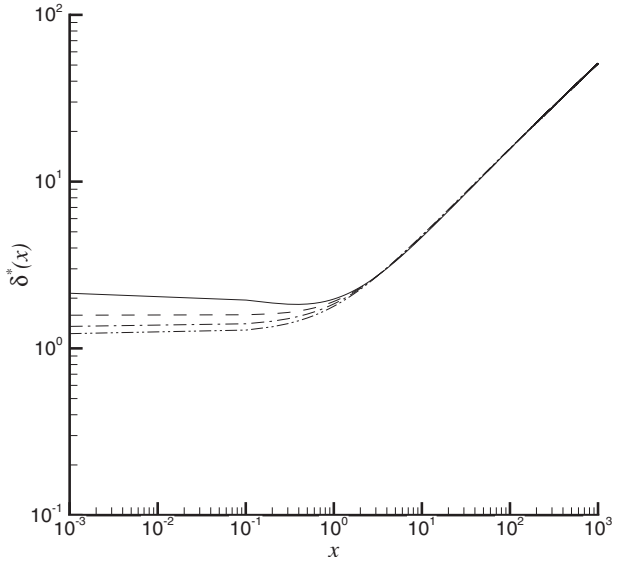

Fig. 10 The 20th-order HAM approximation of $\delta^*(x)$ at different values of α when λ=1/2. Solid line: α=1/4, dashed line: α=1/2, dash-dotted line: α=3/4, and dash-dot-dotted line: α=1.

$$U_w(x) = \sum_{i=1}^{\infty} A_i \left(\frac{x}{1+x} \right)^i \tag{51}$$

is chosen, the resulting governing equation always contains the exact solutions in the whole regions.

5 Conclusions

In this paper, a general analytic approach for nonsimilarity boundary-layer flows of non-Newtonian fluids is proposed by means of an analytic method for highly nonlinear problems, namely, the HAM. The nonsimilarity boundary-layer flows of second-order fluid over a stretching sheet with arbitrary stretching velocity are used as an example to show its validity. Convergent series solutions are obtained for all physical parameters and variables, which agree well with numerical ones. The effects of physical parameters on the skin-friction coefficients and boundary layer thickness are investigated. This example illustrates the validity of the proposed analytic approach.

Unlike perturbation techniques, the HAM is independent of any physical parameters so that it is still valid no matter whether or not a nonlinear problem contains small/large physical parameters. Besides, it provides great freedom to choose different base functions and auxiliary linear operator, using this kind of freedom, we transform the original nonlinear PDE into an infinite number of linear ODEs. More importantly, different from all other analytic techniques, the HAM provides us with a simple way to ensure the convergence of solution series: One can always get accurate enough approximations by means of choosing a proper value of the auxiliary parameter $\hbar$. The analytic approach described in this paper has general meanings and can be applied to solve other types of nonsimilarity boundary-layer flows and heat transfer in general.

Note that, due to the simplicity in mathematics, most researchers are working on similarity boundary-layer flows, which are governed by nonlinear ODEs. However, nonsimilarity flows, which are governed by nonlinear PDEs, are more general and more important in physics, although they are more difficult to solve than similarity flows. We wish that our work can attract more researchers on nonsimilarity flows.

Acknowledgment

Thanks to the anonymous reviewers for their constructive suggestions. This work is partly supported by the National Natural Science Foundation of China (Approval No. 10872129) and the Program for Changjiang Scholars and Innovative Research Team in University (Approval No. IRT0525).

References

[1] Beard, D. W., and Walters, K., 1964, "Elastico-Viscous Boundary Layer Flows," Proc. Cambridge Philos. Soc., **60**, pp. 667–674.
[2] Rajagopal, K. R., Na, T. A., and Gupta, A. S., 1984, "Flow of a Viscoelastic Fluid Over a Stretching Sheet," Rheol. Acta, **23**, pp. 213–215.
[3] Vajravelu, K., and Rollins, D., 1991, "Heat Transfer in a Viscoelastic Fluid Over a Stretching Sheet," J. Math. Anal. Appl., **158**, pp. 241–255.
[4] Vajravelu, K., and Roper, T., 1999, "Flow and Heat Transfer in a Second Grade Fluid Over a Stretching Sheet," Int. J. Non-Linear Mech., **34**, pp. 1031–1036.
[5] Sarma, M. S., and Rao, B. B., 1998, "Heat Transfer in a Viscoelastic Fluid Over a Stretching Sheet," J. Math. Anal. Appl., **222**, pp. 268–275.
[6] Dandapat, B. S., and Gupta, A. S., 1989, "Flow and Heat Transfer in a Viscoelastic Fluid Over a Stretching Sheet," Int. J. Non-Linear Mech., **24**, pp. 215–219.
[7] Pontrelli, G., 1995, "Flow of a Fluid of Second Grade Over a Stretching Sheet," Int. J. Non-Linear Mech., **30**, pp. 287–293.
[8] Cortell, R., 2006, "A Note on Flow and Heat Transfer of a Viscoelastic Fluid Over a Stretching Sheet," Int. J. Non-Linear Mech., **41**, pp. 78–85.
[9] Liao, S. J., 1992, "The Proposed Homotopy Analysis Technique for the Solution of Nonlinear Problems," Ph.D. thesis, Shanghai Jiao Tong University, Shanghai, China.
[10] Liao, S. J., 2003, *Beyond Perturbation: Introduction to the Homotopy Analysis Method*, Chapman and Hall, London/CRC, Boca Raton, FL.
[11] Liao, S. J., 2004, "On the Homotopy Analysis Method for Nonlinear Problems," Appl. Math. Comput., **147**, pp. 499–513.
[12] Liao, S. J., 2005, "A New Branch of Solutions of Boundary-Layer Flows Over an Impermeable Stretched Plate," Int. J. Heat Mass Transfer, **48**, pp. 2529–2539.
[13] Xu, H., Liao, S. J., and Pop, I., 2006, "Series Solutions of Unsteady Boundary Layer of Non-Newtonian Fluids Near a Forward Stagnation Point," J. Non-Newtonian Fluid Mech., **139**, pp. 31–34.
[14] Liao, S. J., and Tan, Y., 2007, "A General Approach to Obtain Series Solutions of Nonlinear Differential Equations," Stud. Appl. Math., **119**, pp. 297–355.
[15] Liao, S. J., 2009, "Notes on the Homotopy Analysis Method: Some Definitions and Theorems," Commun. Nonlinear Sci. Numer. Simul., **14**, pp. 983–997.
[16] Liao, S. J., 2009, "A General Approach to Get Series Solution of Non-Similarity Boundary Layer Flows," Commun. Nonlinear Sci. Numer. Simul., **14**, pp. 2144–2159.
[17] Abbasbandy, S., 2006, "The Application of the Homotopy Analysis Method to Nonlinear Equations Arising in Heat Transfer," Phys. Lett. A, **360**, pp. 109–113.
[18] Sajid, M., Hayat, T., and Asghar, S., 2006, "On the Analytic Solution of the Steady Flow of a Forth Grade Fluid," Phys. Lett. A, **355**, pp. 18–26.
[19] Zhu, S. P., 2006, "An Exact and Explicit Solution for the Valuation of American Put Options," Quant. Finance, **6**, pp. 229–242.
[20] Zhu, S. P., 2006, "A Closed-Form Analytical Solution for the Valuation of Convertible Bonds With Constant Dividend Yield," ANZIAM J., **47**, pp. 477–494.
[21] Yabushita, K., Yamashita, M., and Tsuboi, K., 2007, "An Analytic Solution of Projectile Motion With the Quadratic Resistance Law Using the Homotopy Analysis Method," J. Phys. A, **40**, pp. 8403–8416.
[22] Wu, Y., and Cheung, K. F., 2008, "Explicit Solution to the Exact Riemann Problems and Application in Nonlinear Shallow Water Equations," Int. J. Numer. Methods Fluids, **57**, pp. 1649–1668.
[23] Rajagopal, K. R., 1984, "On the Creeping Flow of the Second Order Fluid," J. Non-Newtonian Fluid Mech., **15**, pp. 239–246.
[24] Hayat, T., and Sajid, M., 2007, "Analytic Solution for Axisymmetric Flow and Heat Transfer of a Second Grade Fluid Past a Stretching Sheet," Int. J. Heat Mass Transfer, **50**, pp. 75–84.
[25] Dunn, J. E., and Rajagopal, K. R., 1995, "Fluids of Differential Type-Critical Review and Thermodynamic Analysis," Int. J. Eng. Sci., **33**, pp. 689–729.
[26] Cebeci, T., and Bradshaw, P., 1984, *Physical and Computational Aspects of Convective Heat Transfer*, Springer-Verlag, New York.
[27] Adomian, G., 1976, "Nonlinear Stochastic Differential Equations," J. Math. Anal. Appl., **55**, pp. 441–452.
[28] Karmishin, A. V., Zhukov, A. T., and Kolosov, V. G., 1990, *Methods of Dynamics Calculation and Testing for Thin-Walled Structures*, Mashionstroyenie, Moscow, in Russian.
[29] Awrejcewicz, J., Andrianov, I. V., and Manevitch, L. I., 1998, *Asymptotic Approaches in Nonlinear Dynamics*, Springer-Verlag, Berlin.
[30] Lyapunov, A. M., 1992, *General Problem on Stability of Motion*, Taylor & Francis, London.